

## PRELIMINARY ANALYTICAL SOLUTIONS OF THE GEOMECHANICAL AND THERMAL STRESSES ON FRACTURE WALLS.

\*Randy R. Koon Koon  
\*\*Indra Haraksingh

Department of Physics  
University of the West Indies  
St. Augustine Campus  
Trinidad

[\\*randykoonkoon88@hotmail.com](mailto:randykoonkoon88@hotmail.com)  
[\\*\\*iharaksingh@yahoo.com](mailto:iharaksingh@yahoo.com)

### **ABSTRACT**

Geothermal energy exploration is heavily dependent on the findings of geophysical surveys and other exploratory methods that yield insight into subsurface characteristics of potential geothermal reservoirs, such as rock morphology, fault lining, and fluid dynamics. Thermal processes not only affect plate tectonics and activities along plate margins but are also responsible for density contrast and changes in rheology. Geothermal systems within the crustal region may appear as liquid- or vapor- dominated systems, as the physics of the water-rock interactions greatly differ from these geological settings.

Building on the understanding of the parallel plate concept, Newtonian fluid flow is described within this system, hence generating a parabolic velocity profile, as this is readily used to capture the understanding of rheology within the crust. However, by considering the geometry of a fracture to be a long thick walled cylinder with axially restrained ends, the paper then seeks to investigate the effect of thermal strains attributed from the geothermal fluids towards the walls of the fracture.

Furthermore, using a general problem or otherwise known as the Lamé problem, which introduces the radial, tangential and axial stresses, and the Hooke's law equations that relates the strains and stresses are modified to accommodate this thermal expansion. Using relevant mathematical approximations, analytical solutions for the respective second order differential equations are obtained and plotted. In addition, using appropriate COMSOL Multiphysics 4.2a modules the deformation of the fracture walls can be modeled.

### **INTRODUCTION**

Geothermal systems are categorized as either conventional or non-conventional resources. A conventional resource is convection dominated as it mainly consists of a hydrothermal system which can be liquid, dry steam or in some cases two phase dominated reservoir. The hydrothermal system is magmatically driven and entails deep circulation of subsurface fluids. On the other hand, a non-conventional resource is conduction dominated and may comprise of a sedimentary basin, a geopressured resource (either liquid or dissolved methane), a radiogenic resource or an engineered geothermal system (EGS).

The paper focuses on conventional type geothermal system which consists of three prime aspects: a young active heat source, permeability and fluid. The system accommodates convective upflow, a low permeability conductively heated cap (smectite rock layer), a continuous/adequate recharge by meteoric waters, and most importantly an outflow of deep circulating fluids (a means of heat transfer) to the surface.

Integrating available data from numerous geoscientific areas yields a conceptual model which draws together consistent interpretation of all such data sets. The paper begins by utilizing the conceptual model of Cumming 2009, as shown in Figure 1. Subsequent from this conceptual model, a stratified cross section of a geothermal system is acquired. Hence a classical andesitic type volcanic system which is closely linked to conventional type geothermal system is used as a basis of the model.

Physical manifestations of stresses in the Earth are represented by fractures. When rock is subjected to these stresses it can be driven beyond its elastic limit.

The rock will deform and soon break, hence resulting in the formation of fractures. A fracture network that enables fluid circulation is as critical an element of a hydrothermal system as are heat and fluid (Kenedi 2010, 2). The paper intends to yield a preliminary insight into a novel approach at producing solutions and describing the physical deformation that the fracture walls experience at different subsurface zones.

**CONCEPTUAL MODEL OF A GEOTHERMAL SYSTEM**

A combination of verbal description and concise graphic that entails pertinent structures and processes which yields insight on existence and feedback on exploitation can be classified as a conceptual model. A typical high-temperature geothermal reservoir with considerable topographic relief is illustrated by Figure 1. This system exhibits characteristic patterns of steam-heated features at a higher regions and chloride springs at lower altitudes.

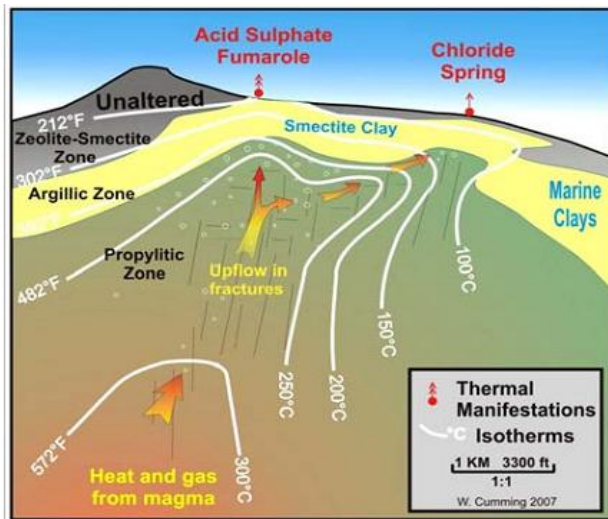


Figure 1: Cross-sectional view of a conceptual model of a 250 to 300°C geothermal reservoir with isotherms, alteration zones, and structures (Source: Cumming 2009).

**Geological Stratification of the Geothermal System**

The cross-sectional view as seen in Figure 1 can be discretized into separate zones. At the point of the smectite clay caprock to the near magmatic lithostatic region, each subsurface level offers its inherent characteristic of the geological structure it entails. Furthermore, five zones each with their respective geologic rock properties can yield a stratified profile

of a typical high-enthalpy geothermal system as seen in Figure 2. These five zones can be categorized as: Argillic, Phyllic, far and near Propylitic, and Near-Magmatic zone.

The argillic zone incorporates the smectite or caprock which acts as the final ingredient in creating a pressurized system. The highly impermeable layer consist of a monoclinic clay-like mineral, in addition, most magnesium minerals are trapped within the smectite rock. Mineral such as quartz, mica an illite can be found within the hydrothermally altered Phyllic zone. The far and near propylitic zone is ideally where the geothermal reservoir exists. The top and bottom of the propylitic zone are lined by epidote which defines the reservoir. The approximate temperature reaches 200 °C and 250 °C for the far and near respectively. It is noted that the permeability is higher within the near propylitic zone as compared the far zone. Finally the near magmatic zone becomes more ductile by nature and biotite, garnet and tourmaline are more readily found within this region.

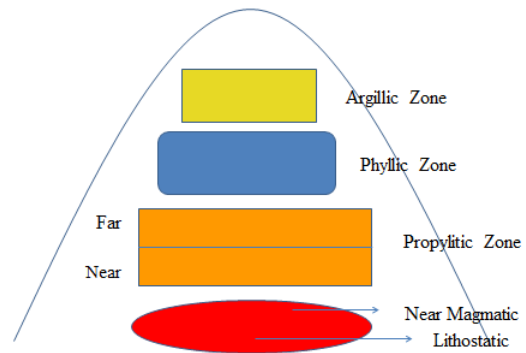


Figure 2: Stratified cross-sectional view of a typical high-enthalpy geothermal system

These zones are highly heterogeneous by nature, consisting of many different minerals. To obtain a general or simplified version the overall zone matrix will then carry characteristics of the dominant rock matrix or mineral found within each zone. This serves a generalization to acquire specific model input values.

**CONCEPTUALIZING THE MODEL**

When considering the geological structure and physical processes occurring within a natural geological system it then becomes highly complex. Notably model results are always interpreted and that the model is merely an approximation of nature. To

facilitate the ease of the geofluid throughout the system, the rock matrix of the hydrothermal reservoir can be considered as highly fractured. Fractured porous rock is generally comprised of a fractured network, a fractured filled network and the matrix blocks between the fractures.

The parallel plate concept (PPC) is a frequently used model for the representation of fractures as shown in Figure 3 below. Through this application it is assumed that the length scale  $l$  (y-axis), of the plates is much greater than the vertical distance between them  $b$  (z-axis,  $l \gg b$ ). Furthermore, hydraulically smooth walls and laminar flow is assumed, corresponding to the Poiseuille fluid model (Wollrath, 1990). In addition, this PPC considers the upper and lower plates to have values of  $Z = +H$  &  $Z = -H$  respectively corresponding to the vertical z-axis. Therefore the vertical displacement between the plates,  $b$ , has a value of  $b = 2H$ .

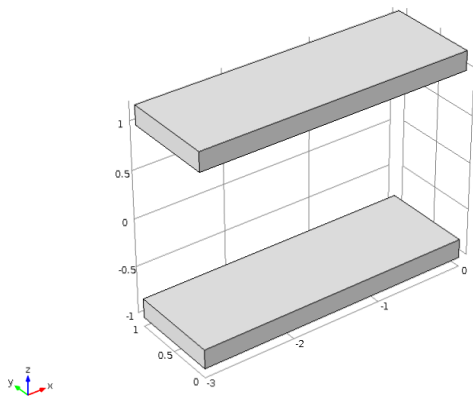


Figure 3: Arbitrary geometric representation of a cross-sectional view of the Parallel Plate Concept (Source: Generated within COMSOL Multiphysics 4.3a).

It can be noted that for an idealized case the fluid will obey the Navier-Stokes equation (NSE) for laminar single-phase flow of an incompressible Newtonian fluid. The fracture model that is being investigated in this thesis is in which the geofluid travels through fracture pathways be it tiny pores of sizable fractures within the rock matrix. Hence the fractures are represented as boundaries between adjacent matrix blocks, hence considered as an interior boundary.

### **Thick-Walled Cylinder**

However, the flow of the geofluid through an arbitrary fracture path can be interpreted as the flow along a thick-walled cylinder as shown in Figure 4

below. With reference to the PPC,  $b$  then becomes the diameter of the inner red cylinder, through which the geothermal fluid is bounded. Ideally the circumference of the inner cylinder acts as a no-slip condition where the velocity of the fluid flow becomes zero. Hence the annulus, represented by the grey portion of the larger cylinder incorporates the space between adjacent fractures. The properties of this annulus mimics that of the overall rock matrix.

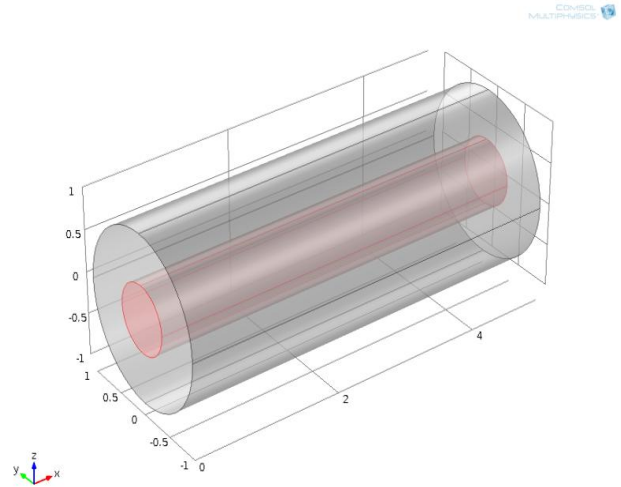


Figure 4: Arbitrary geometric representation of a thick-walled cylinder with an inner tube of flow (Source: Generated within COMSOL Multiphysics 4.3a).

### **Thermal Strain and Deformation**

The geothermal fluid flowing through the inner cylinder will conduct thermal energy to its boundary (circumference of the inner cylinder). Assuming a smooth, laminar flow of fluid through the inner path, heat will be distributed radially at all points along its circumference. The initial temperature  $T_0$ , will exhibit the temperature of the rock matrix within its respective geological stratified zone. The incoming temperature  $T$ , of the geofluid will generate expansion of the surrounding material. Simply the increase in length is proportional to the temperature rise, via a constant of proportionality  $\alpha$ , the coefficient of thermal expansion.

Hence the thermal strain accounted for by the geothermal fluid can be expressed as

$$\epsilon_{thermal} = \alpha(T - T_0) \quad (1)$$

Strain which gives a rate or an extent of deformation is established when the stress forces have the effect of deforming a volume of the material. In addition, the degree to which deformation occurs can be

assumed to be a function of the porosity  $\phi$ , of the geological rock structure. Both the thermal strain and porosity variable are dimensionless and are simply added to the generalized Hooke's law as seen in the proceeding section.

### GENERAL APPROACH TO THE PROBLEM

A generalized approach to understand the system entirely can be performed by envisioning a long cylinder with axially restrained as shown by Figure 4. The differential formulation of the *Lamé Problem* is based on the analysis of the equilibrium of an elementary volume (Giovannozzi, 1990).

A generalization of the problem is performed by accepting the *Lamé Problem*. The fracture is examined as a long cylinder, where every ring of unit thickness measured perpendicular to the plane of the paper is stressed alike. An infinitesimal element of unit thickness is defined by two radii,  $r$  and  $r+dr$  and an angle  $d\phi$ .

The stress components under consideration are  $\sigma_t$  the tangential stress,  $\sigma_r$  the radial stress and  $\sigma_x$  the plane stress. Figure 5, allows the examination of a long cylinder with axially restrained ends. The inner radius is  $r_i$ , and the outer radius is  $r_o$ . The internal pressure of the cylinder generated by the geothermal fluid is given by  $p_i$ , and the external pressure caused by other fluids or tensile stresses is expressed by  $p_o$ . It is important to note that due to symmetry, every element at the same radial distance from the center must be stressed alike, *no shear stress act on the element*.

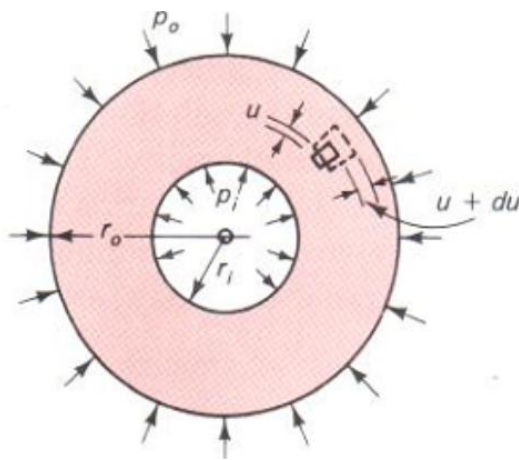


Figure 5: Cross-sectional view of the thick-walled cylinder (Source: Popov 1990, 160)

By considering the thermal strain generated by the geothermal fluid onto the walls of the fracture and the

porosity which will be a function of the matrix porosity, the generalized Hooke's laws relating the stresses and strains can be restated. Hence a classical elasticity solution to the generalized problem proceeds. Using *Lamé Problem* and under Static Equilibrium the following is obtained:

$$\sigma_t - \sigma_r - r \frac{d\sigma_r}{dr} = 0 \quad (2)$$

The strains in the radial and tangential directions are responsible for the deformation of an element. Hence following geometric compatibility  $\epsilon_r$  &  $\epsilon_t$  can be expressed as:

$$\epsilon_r = \frac{du}{dr} \quad (3)$$

$$\epsilon_t = \frac{u}{r} \quad (4)$$

### Properties of Material

As seen in Figure 4, the grey annulus of the thick walled cylinder will experience deformation due to the thermal strain of the geothermal fluid. In addition, the rate or extent of deformation that it undergoes will be a function of the porosity within this region. Therefore, the generalized Hooke's law relating strains to stresses can be restated as shown below:

$$\epsilon_r = \frac{1}{E} (\sigma_r - \nu\sigma_t - \nu\sigma_x) + \alpha\Delta T + \phi \quad (5)$$

$$\epsilon_t = \frac{1}{E} (-\nu\sigma_r + \sigma_t - \nu\sigma_x) + \alpha\Delta T + \phi \quad (6)$$

$$\epsilon_x = \frac{1}{E} (-\nu\sigma_r - \nu\sigma_t + \sigma_x) + \alpha\Delta T + \phi \quad (7)$$

Where E, is Young's Modulus and  $\nu$  is Poisson's ratio. For the case of the thick-walled cylinder with axially restrained deformation, the scenario is one of *plane strain*; hence the axial strain becomes zero, i.e.  $\epsilon_x = 0$ . Equation (7) then simplifies to a relation for the axial stresses as

$$\sigma_x = \nu(\sigma_r + \sigma_t) - \alpha\Delta T - \phi \quad (8)$$

Now applying this result into equations (5) & (6) and solving them simultaneously gives expressions for stresses  $\sigma_r$ , and  $\sigma_t$ , in terms of strains:

$$\sigma_r = \frac{E(\epsilon_r(1-\nu^2) + \epsilon_t(\nu+\nu^2)) - ((\nu+E)(\alpha\Delta T + \phi))(1+\nu)}{(1-\nu^2)^2 - (\nu+\nu^2)^2} \quad (9)$$

$$\sigma_t = (A + B + C / (D - E)^2 \cdot F) + G - H \quad (10)$$

Where:

$$A = E(\epsilon_r(1 - \nu^2) + \epsilon_t(\nu + \nu^2))(1 - \nu^2)$$

$$\begin{aligned}
B &= -v(\alpha\Delta T + \phi)(1 + v) \\
C &= E(\alpha\Delta T + \phi)(1 + v(1 - v^2)) \\
D &= (((1 - v(1 - v^2))^2)^2) \\
E &= (v(1 - v^2) + v(1 - v^2)^2)^2 \\
F &= (v + v^2) \\
G &= (v + E)(\alpha\Delta T + \phi)/v + v^2 \\
H &= E\varepsilon_r/v + v^2
\end{aligned}$$

### Formation of the Differential Equation

At this point the equilibrium equation, (2) can be expressed in terms of one variable  $u$ . Therefore, the strains  $\varepsilon_r$  and  $\varepsilon_t$ , can then be eliminated from equations (9) & (10) as they are expressed in terms of the displacement  $u$  as given by equations (3) & (4). Once the radial and tangential strains are expressed in terms of the displacement, they are finally substituted into equation (2) and simplified, to obtain the desired governing differential equation as shown below:

$$rE\left(\frac{d^2u}{dr^2}\right) - IE\left(\frac{du}{dr}\right) - J\frac{u}{r} - K\frac{u}{r^2} - 2L - rM = 0 \quad (11)$$

Where:

$$I = -2v^2 - v + 1/v + v^2$$

$$J = E(1 - v^2) + (v + v^2)$$

$$K = E(v + v^2)$$

$$L = (v + E)(\alpha\Delta T + \Phi)$$

$$M = (v + E)(\alpha\Delta T + \Phi)(1 + v)$$

Hence the solution to the second order differential equation (ODE) will yield the deformation,  $u$ , in terms of the radius,  $r$ . Since it is a heat conduction problem in a cylindrical system the solutions can be predicted to follow those of the Modified Bessel functions of the first and second kind.

The solution to equation (11) is complex by nature involving both the Bessel I and Bessel K functions and the addition of integrals forms of these functions. It is seen that each of the subsurface stratified geological zones will be associated with its own unique second ODE that will yield the extent of deformation the fracture walls experience at that specified subsurface strata. However, equation (11) can be interpreted to a more exact form by substituting values for the constants by utilizing the table below.

To perform a first approximation, values for the Young's modulus, Poisson's ration, porosity and coefficient of thermal expansion can be acquired from literature. After which a more refined or exact

form of equation (11) is obtain. With reference to Figures 1 and 2, the temperature profiles for each stratified layer are attained. It can be assumed that the temperature of the upflowing geothermal fluid from the high-enthalpy resource is at 325°C. Each zone will carry its associated ambient temperature. The incoming geofluid mixes and yields a subsequent  $\Delta T$  value. Hence it is important to note that for a single layer system (horizontal slice at depth) the temperature will be fixed.

A purely theoretical approach to satisfy this novel approach can be achieved through such a manner. Hence a general form of the solution to equation (11) is given below

$$u(r) = A_1 r^n Bessel I(-A_2)C1 + A_1 r^n Bessel K(-A_2)C2 + A_3 \quad (12)$$

Where C1 & C2 are the constants to solving the ODE since no Initial values were assigned.  $A_1$  and  $A_2$  are exact forms of the solutions.  $A_3$ , however, yields a complex portion of the solution, that of the summation of both modified Bessel I and K, the integral forms of each. For a trivial or simplistic case of the solution to purely determine the form and to gain an understanding of the plots the constants can be placed to one.

By firstly examining equation (11) it does not comply with the conventional differential equation form of the Modified Bessel function. These functions are valid for both a complex argument and purely imaginary arguments. The solutions satisfy this area of imaginary arguments, generating hyperbolic Bessel function of the first and second kind.

### Simulations

This differential equation serves to explain the extent of deformation that occurs within the annulus of the thick-walled system. With the aid of COMSOL Multiphysics 4.3a the differential equation can be coupled with the systems equations to yield a vivid physical description of the extent of deformation along the cavity. However, a general understanding is met by coupling the interfaces, Heat Transfer>Conjugate Heat Transfer>Laminar Flow (nitf) and Structural Mechanics> Solid Mechanics (solid).

The system is idealized by having laminar flow of water within the inner cylinder. With reference to Figure 1, the ambient temperature of zone one or the Argillic zone is on a isotherm of 100 °C. The incoming geofluid retains it arbitrary temperature of 325 °C. Hence the smectite region can be modeled to

illustrated the principal stress or strain that the cavity experiences. It can be noted that along the y and z components of the fracture path the greatest magnitude of force will be applied.

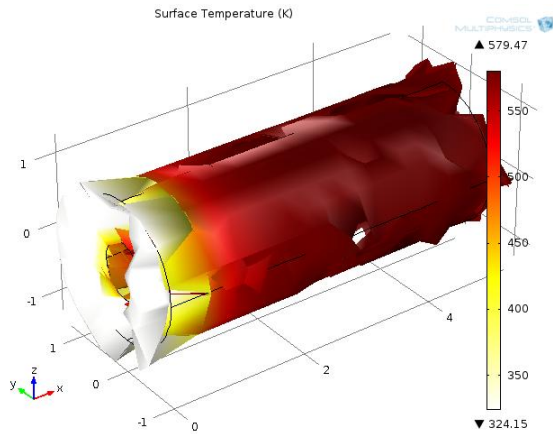


Figure 6: Principal strain in the y-direction of the cavity for Argillic zone (Source: Generated within COMSOL Multiphysics 4.3a).

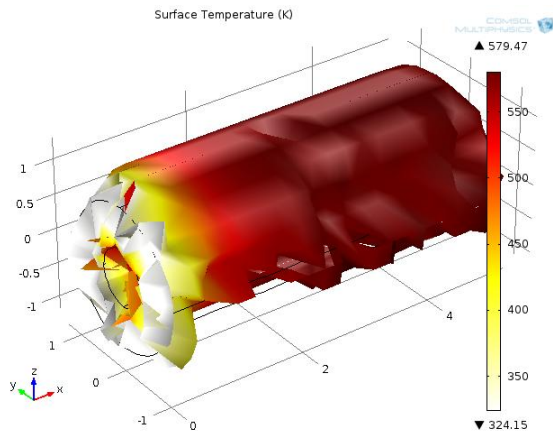


Figure 7: Principal strain in the z-direction of the cavity for Argillic zone (Source: Generated within COMSOL Multiphysics 4.3a).

Within the first third of the cavity length it is seen that the temperature begin to diffuse throughout the system. The inlet experiences an instant deformation and most of the lower portion of the fracture length is disturbed on its exterior as seen in Figures 6 and 7. It is expected that deformation will act the greatest on the inner cylinder.

The outlet of the fracture path can be seen in Figures 8 and 9. Here once again most of the deformation occurs along the z-component of the strain forces. Hence an insight into the deformation of the inner

tube is observed which generates a partial nozzle effect geometry. It is then expected that the velocity profile of the fluid flow path will speed up but also be affect by the collapses an undulating nature that it succumbs to.

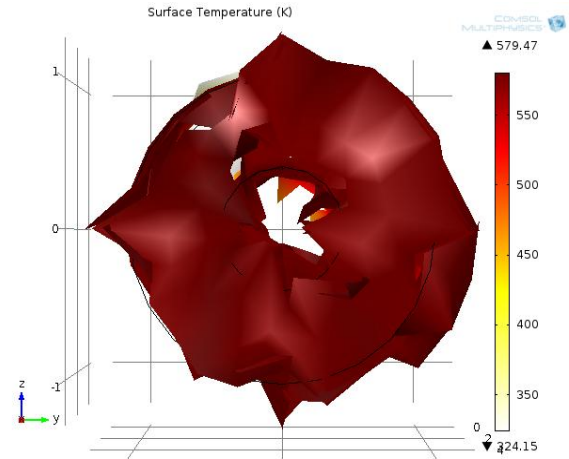


Figure 8: Principal strain in the y-direction of the cavity's outlet within the Argillic zone (Source: Generated within COMSOL Multiphysics 4.3a).

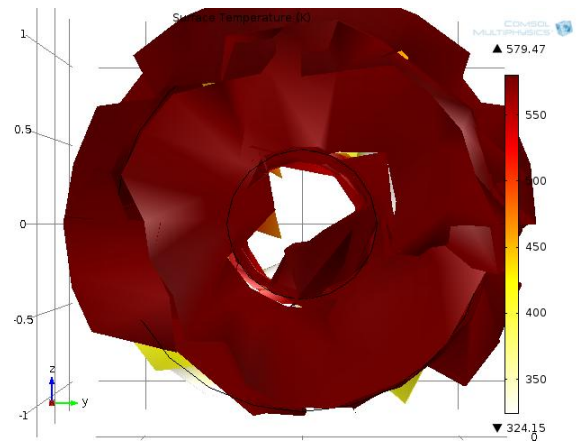


Figure 9: Principal strain in the z-direction of the cavity's outlet within the Argillic zone (Source: Generated within COMSOL Multiphysics 4.3a).

Hence the velocity profile of the geothermal fluid through the fracture is shown in Figures 10 and 11. Smooth concentric circles are not observed Figure 11, rather irregular profiles inscribing the other lower velocity ring are found. An arbitrary valued of 20 m/s was used as the mean inlet velocity. However, it is seen as the profile develops along the fracture path the velocity increases as this is inherent of the 'nozzle effect'. Since the area decrease and the flow rate is fixed the velocity increases.

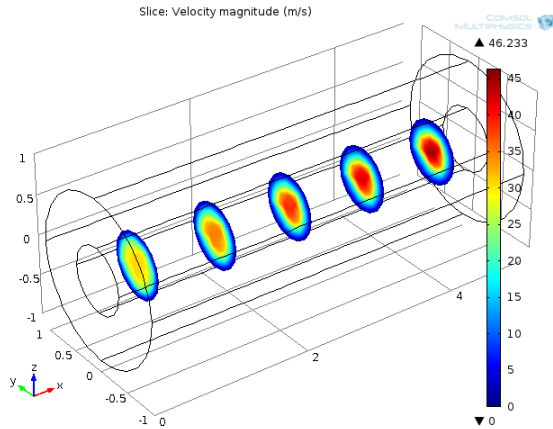


Figure 10: Velocity profile through the cavity within the Argillic zone (Source: Generated within COMSOL Multiphysics 4.3a).

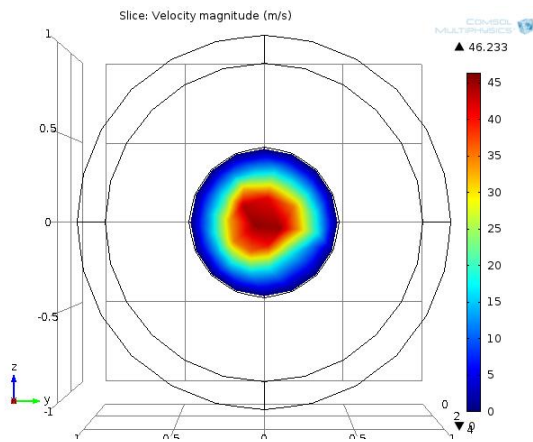


Figure 11: Velocity profile at the cavity's outlet within the Argillic zone (Source: Generated within COMSOL Multiphysics 4.3a).

## LIMITATIONS & FUTURE WORK

Within a high enthalpy geothermal reservoir the deep circulating waters are generally ascribable to the four types: Sodium-chloride, acid-sulfate, sodium-bicarbonate and acid chloride-sulfate waters (Ellis & Mahon, 1977; Henley *et al.*, 1984; Giggenbach, 1988). The geothermal fluid through the Figure 3, was assumed have ideal fluid characteristics. This assumption has limiting effects on the true practical behavior of these fluids.

The validation of this model can be applied with the aid of practical data results. Hence solutions, plots and Equation (11) can be refined by introducing the boundary conditions, the tensile and the compressible forces of pressure on the inner and outer cylinder  $p_i$  and  $p_o$  respectively. Hence the constants C1 and C2

will then yield an accurate form involving  $p_i$  and  $p_o$ . In addition, the verification and the validation of the model can be performed by the implementation of these equations into COMSOL Multiphysics 4.3a interface.

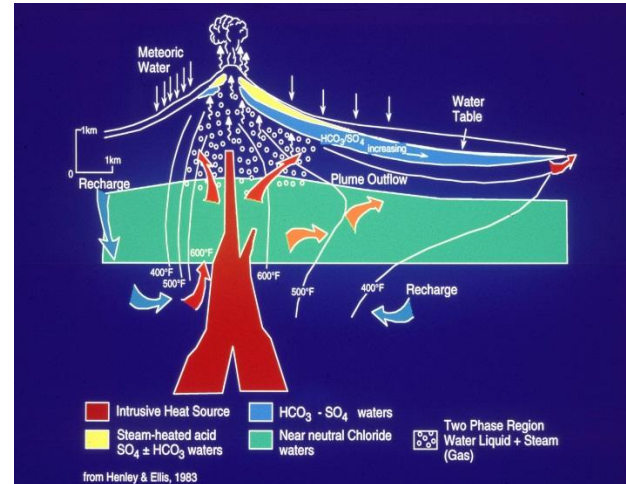


Figure 12: Conceptual model of an Andesitic Volcano (Source: Henley & Ellis 1983).

## REFERENCES

- Cumming, William. 2009. "Geothermal Resource Conceptual Models Using Surface Exploration Data." *Proceedings, 34th Workshop on Geothermal Reservoir Engineering*, Stanford University, Stanford, CA, SGP-TR-187.
- Ellis A.J. and Mahon W.A.J. 1977. *Chemistry and Geothermal Systems*, Academic Press, 392 pp.
- Giggenbach W.F. 1988. Geothermal solute equilibria. Derivation of Na-K-Mg-Ca geothermometers. *Geochim. Cosmochim. Acta* **52**, 2749-2765.
- Giovanozzi R. 1990. *Costruzione di Macchine*, Vol II, Patron-Bologna, Italy.
- Henley R.W., Truesdell A.H., Barton P.B.Jr, Whitney J.A 1984. Fluid-mineral equilibria in hydrothermal systems. *Reviews in Economic Geology* **1**, 267 pp.
- Kenedi, Catherine L. 2010. "Fractures, Faults, and Hydrothermal Systems of Puna, Hawaii, and Montserrat, Lesser Antilles." PhD diss., Duke University.
- Popov, E.P. 1990. *Engineering Mechanics of Solids*. Prentice-Hall, Inc.
- Wollrath, J. 1990. *Ein Strömungs- und Transportmodell für klüftiges Gestein und*

*Untersuchungen zu homogenen  
Ersatzsystemen.* (Institut für  
Strömungsmechanik und Elektronik und  
Elektronisches Rechnen im Bauwesen Hannover,  
Bericht;28) (Zugl.:Hannover, Uni., Diss., 1990).  
Eigenverlag, Hannover.